Inorganic Chemistry

Communication

pubs.acs.org/IC

Simultaneous Presence of Two Different Magnetic Structures in a Single-Crystalline Solid? Hydrogen-Distribution-Dependent Magnetism

Hyun-Joo Koo*,† and Myung-Hwan Whangbo*,‡

†Department of Chemistry and Research Institute for Basic Science, Kyung Hee University (KHU), Seoul 130-701, Republic of Korea

‡Department of Chemistry, North Carolina State University (NCSU), Raleigh, North Carolina 27695-8204, United States

Supporting Information

ABSTRACT: In terms of density functional theory calculations, we explored the reason why the neutron diffraction patterns of a crystalline solid, $NaFe_2(H_3O_2)(MoO_4)_2$, are explained by invoking the simultaneous presence of two widely different magnetic structures. The partitioning into OH and H_2O groups of the "H_3O_2" units, which interconnect FeO_4 chains in each $[Fe_2(H_3O_2)(MoO_4)_2]^-$ layer, leads to various layers different only in their H-atom positions. The crystal structure containing only symmetric $FeO_2(HO)(H_2O)$ chains and that containing only asymmetric FeO_4 chains are found to be responsible for the two observed magnetic structures.

A crystalline solid made up of magnetic ions possesses a unique set of spin-exchange paths and has a unique magnetic structure.[1,2] Thus, it is highly unlikely that a crystalline magnetic solid can exhibit two widely different magnetic structures simultaneously. Nevertheless, precisely such an observation has been reported for $NaFe_2(H_3O_2)(MoO_4)_2$,[3] and the cause for this phenomenon has not been understood yet. In this Communication, we explore the reason for this finding on the basis of density functional theory (DFT) calculations to find that the chemically meaningful structures of $NaFe_2(H_3O_2)(MoO_4)_2$ require the partitioning of H_3O_2 units into H_2O and HO groups and that the spin exchanges of the resulting structures depend on the H-atom distributions, although the Fe/O framework remains unchanged.

In $NaFe_2(H_3O_2)(MoO_4)_2$, the FeO_6 octahedra containing high-spin Fe^{2+} ions share their trans edges to form the FeO_4 chains along the *b* axis (Figure 1a); these chains are interlinked by the MoO_4 tetrahedra and H_3O_2 bridges to form layers of stoichiometry $[Fe_2(H_3O_2)(MoO_4)]^-$ parallel to the *ab* plane with two FeO_4 chains per unit cell along the *a* axis, and these layers are stacked along the *c* direction with Na^+ between the layers (Figure 1b). The neutron diffraction patterns of $NaFe_2(D_3O_2)(MoO_4)_2$ below its long-range antiferromagnetic (AFM) ordering temperature of 17 K are explained if it is assumed that two widely different magnetic structures with the propagation vectors $q_1 = (0, 0, 0)$ and $q_2 = (0, 0, {}^1/_2)$ coexist simultaneously. In the q_1 structure, the spins in each FeO_4 chain along the *b* axis have ferromagnetic (FM) coupling, and adjacent FeO_4 FM chains have AFM coupling along the *a* axis but FM coupling along the *c* axis (Figure 2a). In the q_2 structure, the spins

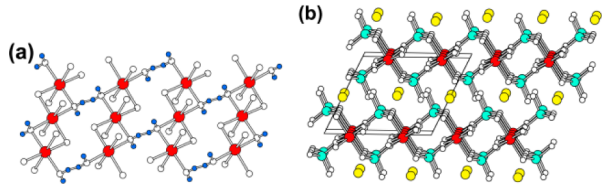

Figure 1. (a) Layer of the FeO_4 chains in the *ab* plane. For simplicity, the MoO_4 tetrahedra bridging adjacent FeO_4 chains are not shown. The red, medium white, and small blue circles represent the Fe, O, and H atoms, respectively. (b) View of $NaFe_2(H_3O_2)(MoO_4)_2$ approximately along the *b* axis, where the H_3O_2 units are not shown for simplicity. The cyan and yellow circles represent the Mo and Na atoms, respectively.

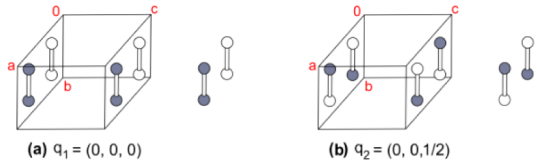

Figure 2. Two magnetic structures of $NaFe_2(H_3O_2)(MoO_4)_2$ with propagation vectors (a) q_1 and (b) q_2.

in each FeO_4 chain have AFM coupling, and adjacent FeO_4 AFM chains have AFM coupling along the *a* and *c* axes (Figure 2b). It is remarkable that the intrachain Fe−O−Fe superexchange is AFM in the q_2 structure but is FM in the q_1 structure, despite the fact that the Fe/O framework is identical in both structures. Because ∠Fe−O−Fe of the edge-sharing FeO_4 chains is considerably greater than 90° (i.e., 98.8°),[3] one would have expected that the FeO_4 chains should be AFM chains on the basis of the Goodenough rule.[4] This is not true for the q_1 structure. Thus, it is necessary to quantitatively evaluate the spin exchanges of $NaFe_2(H_3O_2)(MoO_4)_2$, which we carry out by performing energy-mapping analysis[1,2] based on DFT calculations.

A key to resolving the magnetic properties of $NaFe_2(H_3O_2)(MoO_4)_2$ lies in the "H_3O_2" units of $NaFe_2(H_3O_2)(MoO_4)_2$, which "link" adjacent FeO_4 chains in the *ab* plane (Figure 1a). Each H_3O_2 unit linking adjacent FeO_4 chains occurs when the HO−H + H−O groups are superposed onto the O−H + H−OH groups. The H···H distance between H_2O and HO in each H_3O_2 unit is only 0.910 Å. Given 1.20 Å as the van der Waals radius of H, the nonbonded H···H distance should be greater than ∼2.40

Received: August 16, 2014
Published: September 29, 2014

   dx.doi.org/10.1021/ic502003j | *Inorg. Chem.* 2014, 53, 10800−10802

Å. Thus, each H_3O_2 unit should be partitioned into H_2O and HO groups to obtain the chemically meaningful crystal structure $NaFe_2(H_2O)(HO)(MoO_4)_2$. This partitioning can generate a large number of different layer structures. For simplicity, let us consider only the two ideal layer structures, namely, a layer of asymmetric FeO_4 chains (model 1 layer) depicted in Figure 3a

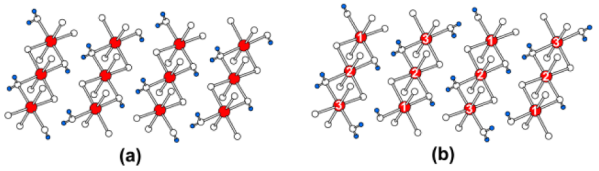

Figure 3. Layers of (a) asymmetric FeO_4 chains and (b) symmetric FeO_4 chains in the *ab* plane. The MoO_4 tetrahedra bridging adjacent FeO_4 chains are not shown.

and that of symmetric FeO_4 chains (model 2 layer) depicted in Figure 3b. In the model 1 layer, all Fe sites are identical because they all form an identical $FeO_4(H_2O)(HO)$ octahedron. In the model 2 layer, there occur three different Fe sites, say, Fe(1), Fe(2), and Fe(3), which form $Fe(1)O_4(HO)_2$, $Fe(2)O_4(H_2O)(HO)$, and $Fe(3)O_4(H_2O)_2$ octahedra, respectively. We probe whether these two layers, which differ only in their H-atom positions, possess different magnetic structures that can account for the magnetic structures reported for $NaFe_2(H_3O_2)(MoO_4)_2$ by constructing two model structures of $NaFe_2(H_2O)(HO)(MoO_4)_2$, one made up of only the model 1 layers and the other consisting of only the model 2 layers [hereafter referred to as the model 1 and 2 structures, respectively].

For the spin-exchange interactions of the model 1 structure, we consider the three spin-exchange paths J_1–J_3 in each layer (Figure 4a), and for those of the model 2 structure, the six spin-

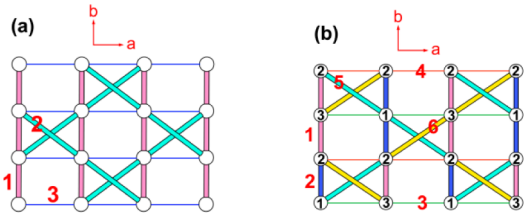

Figure 4. Spin-exchange paths in the layers of (a) the asymmetric FeO_4 chains of the model 1 structure and (b) the symmetric FeO_4 chains of the model 2 structure. Here the numbers 1–6 refer to the spin exchanges J_1–J_6, respectively.

exchange paths J_1–J_6 in each layer (Figure 4b). For the model 1 structure, we also consider the interlayer exchange J_4 [see Figure S1 of the Supporting Information (SI)]. In the model 2 structure, there are a large number of nonequivalent interlayer spin-exchange paths because each FeO_4 chain has three nonequivalent Fe atoms. In addition, the interlayer separation is very large. In such a case, the interlayer spin exchanges become too weak to be reliably evaluated by DFT calculations, so they were not examined. Notice that J_1 of Figure 4a as well as J_1 and J_2 of Figure 4b are Fe–O–Fe superexchanges, while the rest are Fe–O···O–Fe supersuperexchanges.

To determine the values of J_1–J_4 of the model 1 structure, we consider the five ordered spin states presented in Figure S2 of the SI. To evaluate the spin exchanges J_1–J_6 of the model 1 structure, we consider the seven ordered spin states shown in Figure S3 of the SI. The relative energies of these ordered spin states are determined on the basis of DFT electronic structure calculations by employing the projected augmented-wave method encoded in the Vienna ab initio simulation package[5] and the generalized gradient approximation of Perdew, Burke, and Ernzerhof[6] for the exchange-correlation corrections, the plane-wave cutoff energy of 700 eV, and the threshold of self-consistent-field energy convergence of 10^{-6} eV. The irreducible Brillouin zone was sampled with 16 *k* points. To describe the electron correlation associated with the Fe 3d states, the DFT plus on-site repulsion U (DFT+U) calculations[7] were carried out with effective $U^{eff} = U - J = 3$, 4, and 5 eV on the Fe atom. The relative energies of the ordered spin states determined from these DFT+U calculations are summarized in Tables S1 and S2 of the SI. To extract the values of the spin exchanges from these calculations, we employ energy-mapping analysis,[1,2] in which the total spin-exchange energies of the ordered spin states are expressed in terms of the spin-exchange Hamiltonian

$$\hat{H} = -\sum_{i<j} J_{ij}\vec{S}_i\cdot\vec{S}_j \qquad (1)$$

where J_{ij} is the spin-exchange parameter for the interaction between the spin sites *i* and *j* ($J_{ij} = J_1$–J_4 for the model 1 structure, and $J_{ij} = J_1$–J_6 for the model 2 structure). Our DFT+U calculations show that the Fe^{2+} ions of the model 1 and 2 structures have moments of ~3.7 μ_B and hence exist as high-spin Fe^{2+} ($S = 2$) ions. Thus, the total spin-exchange energies per four formula units are written as summarized in the SI. By mapping the energy differences between the ordered spin states obtained from the DFT+U calculations onto the corresponding energy differences obtained from the spin Hamiltonian, we obtain the values of the spin exchanges summarized in Table 1.

Table 1. Spin-Exchange Parameters (in k_BK) Obtained from DFT+U Calculations for the Model 1 and 2 Structures of $NaFe_2(H_2O)(HO)(MoO_4)_2$

	U (eV)		
	3	4	5
(a) Model 1 Structure			
J_1	−25.1	−18.3	−13.2
J_2	−3.7	−3.5	−2.7
J_3	−4.5	−4.3	−3.5
J_4	−0.1	−0.08	−0.06
(b) Model 2 Structure			
J_1	+40	+36	+38
J_2	+41	+32	+45
J_3	−42	−35	−37
J_4	+3	+8	+6
J_5	−51	−30	−43
J_6	−42	−30	−31

For the model 1 structure, Table 1a shows that J_1–J_4 are all AFM, with the relative strength decreasing in the order $|J_1| \gg |J_3| > |J_2| \gg |J_4|$. The intrachain spin exchange J_1 makes the spins of each FeO_4 chain along the *b* axis antiferromagnetically coupled. Each exchange triangle (J_1–J_3) between adjacent chains is spin-frustrated, but J_3 is stronger than J_2, so that adjacent FeO_4 AFM chains become antiferromagnetically coupled along the *a* axis. This interchain AFM coupling does not double the *a* axis because there are two FeO_4 AFM chains per unit cell along the *a* axis. The interlayer exchange J_4 is AFM, although weakly, and doubles the *c* axis. Therefore, the spin-exchange interactions of the model 1

dx.doi.org/10.1021/ic502003j | Inorg. Chem. 2014, 53, 10800–10802

structure are consistent with the q_2 = (0, 0, $^1/_2$) magnetic structure (Figure 2b). For the model 2 structure, Table 1b shows that the intrachain exchanges J_1 and J_2 are both FM, so the spins of each FeO_4 chain along the b axis are ferromagnetically coupled. The interchain exchange J_4 is very weakly FM, while J_3, J_5, and J_6 are all substantially AFM. Therefore, the FeO_4 FM chains are antiferromagnetically coupled along the a axis. Consequently, the intralayer spin-exchange interactions of the model 2 structure are in agreement with the q_1 = (0, 0, 0) magnetic structure (Figure 2a).

Thus, our quantitative mapping analysis shows that the nature of the spin exchanges in the $[Fe_2(H_3O_2)(MoO_4)]^-$ layer depends on the H-atom distribution in the FeO_4 chains and, in particular, that the Fe−O−Fe superexchange is FM in the model 2 structure despite the fact that ∠Fe−O−Fe is considerably greater than 90°. It is of interest to consider a qualitative reason for this apparently surprising observation. Between the two spin sites i and j described by magnetic orbitals ϕ_i and ϕ_j, respectively, the spin exchange has FM and AFM contributions that increase with the overlap density $\phi_i\phi_j$ and the overlap integral $\langle\phi_i|\phi_j\rangle$, respectively.[1,2] It is the O 2s/2p orbitals (i.e., the tail parts) of the magnetic orbitals that determine the magnitudes of $\phi_i\phi_j$ and $\langle\phi_i|\phi_j\rangle$. When the Fe^{2+} spin sites become nonequivalent by having different numbers of O, HO and H_2O ligands, the changes in the magnetic orbitals occur largely in their tail parts (in local shape and symmetry). Thus, an overlap integral $\langle\phi_i|\phi_j\rangle$ can become diminished without much reduction of the overlap density $\phi_i\phi_j$. In each FeO_4 chain of the model 1 structure, every adjacent pair of Fe atoms are identical (Figure 3a), which favors AFM interactions. In each FeO_4 chain of the model 2 structure, however, every two adjacent Fe atoms are nonequivalent (Figure 3b), which favors FM interactions.

As already noted, spin frustration between adjacent FeO_4 chains exists in the model 1 structure but is absent in the model 2 structure. This accounts for the presence of spin canting in the q_2 magnetic structures but its absence in the q_1 magnetic structure (see the SI for details). This provides additional support for our quantitative analysis.

An important implication of our analysis should be noted. In principle, the partitioning of each H_3O_2 unit into the HO and H_2O groups can generate many different structures for the $[Fe_2(H_2O)(HO)(MoO_4)_2]^-$ layer without any long-range order. If this were the case, there would be no well-defined magnetic reflections in neutron diffraction measurements. Because the neutron diffraction patterns of $NaFe_2(H_3O_2)(MoO_4)_2$ below 17 K are well described by assuming the coexistence of the q_1 and q_2 magnetic structures and because the q_1 and q_2 structures are well described by the model 2 and 1 structures, respectively, it is compelling that the as-prepared samples of $NaFe_2(H_3O_2)(MoO_4)_2$ consist of microdomains of the model 1 and 2 crystal structures.

In summary, the simultaneous coexistence of two different magnetic structures reported for $NaFe_2(H_3O_2)(MoO_4)_2$ is explained by the model 1 and 2 crystal structures arising from the partitioning of H_3O_2. It is of interest that the nature of the intrachain Fe−O−Fe superexchange, with ∠Fe−O−Fe much greater than 90°, can switch from AFM to FM depending on the H-atom distributions in the FeO_4 chains. It would be of importance to verify experimentally our conclusion that $NaFe_2(H_3O_2)(MoO_4)_2$ should consist of microdomains of these two structures.

■ ASSOCIATED CONTENT

Supporting Information

Tables S1−S3, Figures S1−S5, description of energy-mapping analysis for the spin exchanges, and spin-canting analysis. This material is available free of charge via the Internet at http://pubs.acs.org.

■ AUTHOR INFORMATION

Corresponding Authors

*E-mail: hjkoo@khu.ac.kr.

*E-mail: mike_whangbo@ncsu.edu.

Notes

The authors declare no competing financial interest.

■ ACKNOWLEDGMENTS

The work at KHU was supported by Basic Science Research Program through the National Research Foundation of Korea funded by the Ministry of Education, Science and Technology (Grant 2010-0021042). This research was supported by the computing resources of the NERSC Center and HPC Center of NCSU.

■ REFERENCES

(1) Whangbo, M.-H.; Koo, H.-J.; Dai, D. *J. Solid State Chem.* **2003**, *176*, 417−481.

(2) Xiang, H. J.; Lee, C.; Koo, H.-J.; Gong, X. G.; Whangbo, M.-H. *Dalton Trans.* **2013**, *42*, 823−853.

(3) Maalej, W.; Vilminot, S.; André, G.; Elaoud, Z.; Mhiri, T.; Kurmoo, M. *Inorg. Chem.* **2011**, *50*, 9191−9199.

(4) Goodenough, J. B. *Magnetism and the Chemical Bond*; Robert E. Krieger Publishing Company: Huntington, NY, 1976.

(5) (a) Kresse, G.; Hafner, J. *Phys. Rev. B* **1993**, *47*, 558−561. (b) Kresse, G.; Furthmüller, J. *Comput. Mater. Sci.* **1996**, *6*, 15−50. (c) Kresse, G.; Furthmüller, J. *Phys. Rev. B* **1996**, *54*, 11169−11186.

(6) Perdew, J. P.; Burke, S.; Ernzerhof, M. *Phys. Rev. Lett.* **1996**, *77*, 3865−3868.

(7) Dudarev, S. L.; Botton, G. A.; Savrasov, S. Y.; Humphreys, C. J.; Sutton, A. P. *Phys. Rev. B* **1998**, *57*, 1505−1509.